Identity Hydrogen Abstraction Reactions, $X^{\bullet} + H-X' \rightarrow X-H + X'^{\bullet}$ ($X = X' = CH_3$, SiH_3, GeH_3, SnH_3, PbH_3): A Valence Bond Modeling

Sason Shaik,*,† Wei Wu,*,‡ Kunming Dong,‡ Lingchun Song,‡ and Philippe C. Hiberty§

Department of Organic Chemistry and the Lise Meitner-Minerva Center for Computational Quantum Chemistry, The Hebrew University, Jerusalem 91904, Israel, Department of Chemistry and State Key Laboratory for Physical Chemistry of Solid Surfaces, Xiamen University, Xiamen, Fujian 361005, P. R. of China, and Laboratoire de Chimie physique, Groupe de Chimie Théorique, Université de Paris-Sud, 91405 Orsay Cédex, France

Received: April 3, 2001; In Final Form: June 26, 2001

Breathing orbital valence bond (BOVB) computations (Hiberty, P. C.; Humbel, S.; Archirel, P. *J. Phys. Chem.* **1994**, *98*, 11697) are used to obtain identity barriers for hydrogen transfer reactions between X groups, X = H, CH_3, SiH_3, GeH_3, SnH_3, and PbH_3. Modeling of these barriers by means of VB state correlation diagrams (Shaik, S.; Shurki, A. *Angew. Chem.* **1999**, *38*, 586) lead to simple expressions for the barriers (eqs 21 and 22). These expressions show that the organizing quantity of the barriers is the singlet−triplet excitation energy (ΔE_{ST}) or bond energy (D) of the X−H bond that undergoes activation. The larger the ΔE_{ST} or D, the higher the identity barrier. These equations are successfully applied to deduce barriers for hydrogen transfers between electronegative groups, X = X′ = F, Cl, Br, and I. The "polar effect" (Russell, G. A. In *Free Radicals*; Kochi, J. K., Ed.; Wiley: New York, 1973; Vol 1, p 293−298) is shown to be significant but virtually constant in the series. Thus, identity processes mask the polar effect which is more clearly expressed in nonidentity hydrogen transfer reactions. Generalization of the model to other atom transfer reactions is discussed.

One of the most fundamental reactions of radicals is hydrogen abstraction. On the one hand, this is a simple enough process to draw a great deal of basic research. On the other hand, its added allure is its association with DNA-damaging, destruction of cell membranes, aging, Alzheimer's disease, oxidation of organic molecules by metallo-enzymes, and so on.[1] As such, the field of hydrogen abstraction has become an arena of considerable practical and theoretical research, aimed at understanding the reactivity patterns of these reactions. Important correlations were established with fundamental factors, such as the bond energy, steric effects, and the "polar effect". The latter effect is related to the charge polarization in the transition state.[2,3] Nevertheless, there is still a need for a unifying model which can reveal trends and make predictions in a systematic manner. A key toward unification is the understanding of the identity process, where the hydrogen is transferred between two identical groups, X = X′, in eq 1:

$$X^{\bullet} + H-X' \rightarrow X-H + X'^{\bullet} \qquad (1)$$

The barrier of identity reactions has a pure kinetic origins, and therefore, its modeling is a key step in any theoretical treatment.

It is reasonable to expect that the successful models will be those which involve a clear mechanism of barrier formation associated with compact expressions of the barrier and its dependence on fundamental properties of the reactants. Such models already exist and describe barrier formation in terms of state-crossing[4] and valence bond (VB) configuration mixing,[5−10] etc.[11] Nevertheless, all of the existing models have a way to go toward the desired goal of unification, and there still seems to be disagreement between them on the important factors of reactivity. Is it the polar effect that dominates trends in the identity barriers or is it the bond energy of or the singlet−triplet excitation of the H−X bond that is broken and remade in the identity process?[4,5] As a step along the way, we decided to apply ab initio VB computations of trends in the barriers of identity hydrogen transfer reactions. Previous VB computations were limited to X = X′ = H[6−8] and to X = X′ = F.[6] Here we extend the VB study to group IV radicals, X = X′ = CH_3, SiH_3, GeH_3, SnH_3, and PbH_3, and compare the results with the most elementary reaction of the family, for X = X′ = H.[12] The reaction for X = CH_3 was investigated experimentally, and its barrier is known.[13,14] Nonidentity hydrogen abstraction by $X^{\bullet}$ = $H^{\bullet}$ and H−X′ = SiH_4 and GeH_4 are important processes in interstellar atmospheres and in the semiconductor industry.[15] R_3Sn-H is a useful reagent, which participates in hydrogen transfer in organic syntheses. Thus, the reaction series in eq 1 has also relevance to practical processes. The present paper aims, therefore, to quantify by means of VB computations the various factors of reactivity in the identity series, the bond energy, the singlet−triplet excitation, and the polar effect; to weigh their relative importance; and establish the organizing quantities that dominate all of the computed trends. The barriers will then be modeled by means of VB diagrams[9,10] and compact expressions will be derived. The so derived barrier expressions will be tested by application to other reactions where the polar effect should be strong ($X = X' =$ F, Cl, Br, and I).

Theoretical Methods

The potential energy profile can be constructed by mixing of VB structures along the reaction coordinate.[10] The compact model uses VB state correlation diagrams (VBSCDs)[10] exempli-

* To whom correspondence should be addressed.
† The Hebrew University.
‡ Xiamen University.
§ Université de Paris-Sud.

10.1021/jp011251c CCC: $20.00 © 2001 American Chemical Society
Published on Web 08/15/2001

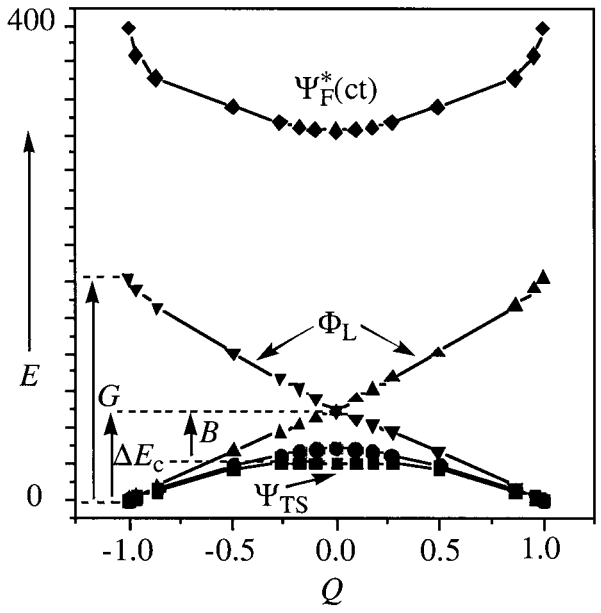

Figure 1. Typical VBSCD for $X^{\bullet} + H-X' \rightarrow X-H + {}^{\bullet}X'$ exemplified for $X = CH_3$. The Lewis curves are annotated with triangles, and the Lewis states nascent of their avoided crossing are shown with bold circles. The final adiabatic state which involves the mixing of the charge transfer states, $\Psi_F^*(ct)$, is annotated with bold squares. The crossing point is indicated by the star and its height is given by ΔE_c. Shown also is the resonance energy of the transition state, *B*, and the promotion gaps, *G*.

fied in Figure 1 with one of the target reactions, in eq 1 ($X = X' = CH_3$). The coordinate Q is defined as the bond order difference:

$$Q = n_1(d_1) - n_2(d_2); \quad n(d) = e^{-a(d-d_0)} \tag{2}$$

where $n(d)$ is calculated for any given distance (d) relative to the equilibrium distance (d_0) of X−H. The constant a is conveniently chosen so as to make the n value equal 0.5 at the transition state (with no implications on questions related to "conservation of bond order").[8]

The barrier arises because of the avoided crossing of two state curves, called the Lewis curves (labeled with triangles), which correspond to the bonds that interchange during the transformation. The barrier is given as

$$\Delta E^{\ddagger} = fG - B \tag{3}$$

where f is some fraction of the promotion gap, G, that separates the two Lewis curves at their onset ($Q = \pm 1$). The quantity B is the resonance energy of the transition state (the curve labeled with squares), which is contributed in part by the avoided crossing of the two Lewis curves and in part by the mixing of excited states not associated with the bond breaking and bond formation and, hence, called foreign excited state, Ψ_F^*. The foreign excited state in Figure 1 is the curve decorated with diamonds. As explained later, it corresponds to the charge transfer state. The VBSCDs and respective quantities are computed by means of ab initio VB methods.

VB Procedures. In VB theory, a state wave function, Ψ is given as a linear combination of VB structures, Φ_i, in eq 4:

$$\Psi = \Sigma_i c_i \Phi_i \tag{4}$$

The VB structures correspond to all of the modes of distributing the "active electrons" which participate in the interchanging bonds. In the case of hydrogen transfer, there are three electrons to distribute in the orbitals which define the interchanging bonds along the X−H−X′ axis. These are the active electrons and orbitals which are treated in a VB manner. The rest of the occupied orbitals (the inactive part) are treated as electron pairs in doubly occupied orbitals.

In the VBSCF method,[6] one optimizes the coefficients as well as the orbitals which constitute the VB structures. The orbitals are optimized as a common set for all of the VB structures. In the BOVB method,[16] the orbitals are allowed to be different for each VB structure. In this manner, the orbitals respond to the instantaneous field of the individual VB structure rather than to an average field of all of the structures. As such, the BOVB method accounts for part of the dynamic correlation, while leaving the wave function compact. The BOVB method is quantitatively more accurate than VBSCF, even though BOVB and VBSCF wave functions look generally very similar.

A compact VB method, which is partway between VBSCF and BOVB, is BDOVB which describes each bond in a single structure with bond distorted orbitals (BDOs)[17] that are semilocalized atomic orbitals with delocalization tails, like the ones used in GVB and SCVB methods,[18,19] with the exception that the delocalization tails of the BDO are constrained to the bonded atoms in a given VB structure. Thus, by allowing the BDOs to delocalized over X and H, one describes the Lewis X−H bond, whereas by allowing them to delocalize over H and X′, one describes the H−X′ bond. Because the BDOs and other orbitals are freely optimized, the BDOVB method involves some of the dynamic correlation of the BOVB method but is again quantitatively less accurate.

The final and best results are presented at the BOVB level. It must be remembered though that the BOVB wave function is very compact and therefore its accuracy is expected to be less than those of extensively correlated MO-based methods. The merit of the VB calculation is its lucidity, whereas its numerical accuracy should be assessed against the trends rather than the individual numbers.

The weights of the VB structures were determined by use of the Coulson−Chirgwin[20] formula, eq 5, which is the equivalent of a Mulliken population analysis in VB theory:

$$w_i = c_i^2 + \Sigma_{j \neq i}[c_i c_j \langle \Phi_i | \Phi_j \rangle] \tag{5}$$

The calculations used the 6-31G* basis set for $X = H$, CH_3, and SiH_3. For SiH_3 and the heavier analogues, we used the Los Alamos effective core potential and matching basis set, LANL2DZ, to which we added d polarization functions taken from 6-31G* (henceforth ECP/31G*). To benchmark the VB results, we carried out MP2 and CCSD(T) calculations for all of the reactions. The VB calculations were done with the Xiamen package of programs.[21] The MP2 and CCSD(T) calculations were carried out using Gaussian 98.[22]

VB Structures Set. The VB structures for a hydrogen transfer reaction are shown in Scheme 1. All of the structures involve three electrons, which are distributed among the three fragments in all possible ways. Two of the structures are covalent and describe the covalent spin pairing in either the right-hand or left-hand bond of the reactants (r) and products (p), respectively. These structures are labeled as $\Phi_{HL}(r)$ and $\Phi_{HL}(p)$ where the subscript HL refers to names of Heitler and London who introduced this wave function in their seminal study.[23] Other structures are ionic and labeled as Φ_i with parenthetical designators which indicate whether they contribute to the bonds of the reactants and products (r and p) or are only excited states (ex).

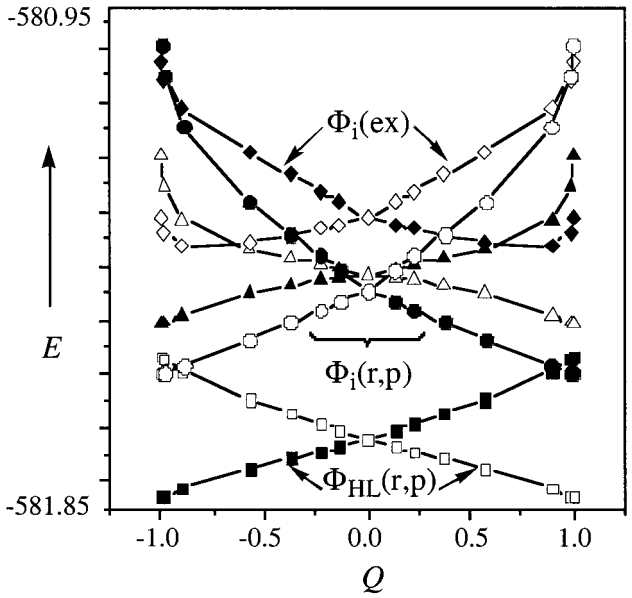

Figure 2. Energy variation of the VB structures along the reaction coordinate *Q*.

SCHEME 1: VB Structure Set for Identity Hydrogen Transfer Reactions, X• + H−X′ → X−H + •X′

Φ_{HL}(r,p)

X· H·—·X′ X·—·H ·X′

1 **2**

Φ_i(r,p)

X· H^+ $:X'^-$ X· $H:^-$ X'^+

3 **4**

$X:^-$ H^+ ·X′ X^+ $:H^-$ ·X′

5 **6**

Φ_i(ex)

X^+ H· $:X'^-$ $X:^-$ H· X'^+

7 **8**

A typical plot of the energies of these structures along the reaction coordinate *Q* is exemplified in Figure 2 (using VBSCF data for X = CH_3). It is apparent from Figure 2 that the HL structures intersect one another along *Q*. Further, it is seen that all other six ionic structures are substantially higher than the HL ones, at $Q = 0$ and ± 1. This is a typical situation *for all of the series studied here*.

Formation of Lewis Curves from the VB Structures. To convert Figure 2 into a compact VBSCD shown above in Figure 1, we need to mix the covalent HL structures with the corresponding ionic structures which are required to describe a two-electron Lewis bond. Thus, mixing of $\Phi_{HL}(r)$ with $\Phi_i(r)$ structures **3** and **4** leads to the right-hand side H−X′ Lewis bond for the reactant X•/H−X′. Similarly, mixing of $\Phi_{HL}(p)$ with $\Phi_i(p)$ structures **5** and **6** leads to the Lewis bond of the product, X−H/•X′. Subsequently, the two Lewis curves are computed by tracing along *Q* the optimized VB structure given by eqs 6a and 6b:

$$\Phi_L(r) = c_1\Phi_{HL}(r) + c_3\Phi_i(r; \mathbf{3}) + c_4\Phi_i(r; \mathbf{4}) \quad (6a)$$

$$\Phi_L(p) = c_2\Phi_{HL}(p) + c_5\Phi_i(p; \mathbf{5}) + c_6\Phi_i(p; \mathbf{6}) \quad (6b)$$

The Lewis structures can be optimized at the VBSCF or BOVB levels. Alternatively, use of BDOs can lead to a compact description of the Lewis structures. Thus, the BDOs of the Lewis structure, $\Phi_L(r)$, involve delocalization tails on the right-hand side X′ and on the H, whereas the active orbital of X is strictly localized on this center, resulting in X•/H−X′. Similar but mirror image description pertains to the BDOs in $\Phi_L(p)$, which result in X−H/•X′.

From Lewis Curves to the VBSCD. The remaining structures, $\Phi_i(ex)$, **7** and **8**, correlate with the charge-transfer excited states of the Lewis structures. For example, in one extreme of *Q*, structure **7** is the charge transfer state $X^+/(HX')^-$, and in the other *Q* extreme, it is the charge transfer state, $(XH)^+/:X'^-$. Structure **8** is the mirror image of structure **7**. These structures do not contribute to the nature of the bonds in the ground states and, as such, do not belong to the Lewis curves. They can however be grouped into a single excited-state curve, called the "foreign excited state", Ψ_F*.[10] In our case, we add the charge transfer designator to specify the nature of this "foreign state", Ψ_F*(ct), defined in eq 7:

$$\Psi_F^*(ct) = c_7\Phi_i(ex; \mathbf{7}) + c_8\Phi_i(ex; \mathbf{8}) \quad (7)$$

The compact diagram VBSCD was already exemplified above in Figure 1, for X = CH_3, which is prototypical for all of the reactions studied here. The Lewis structures, Φ_L (shown with triangles), intersect along the coordinate *Q*, whereas the energy of the excited-state curve (decorated with diamonds), Ψ_F*(ct), varies basically horizontally above the two principal curves. The two Lewis curves mix and avoid their crossing generating a lower energy curve, which is the resonating Lewis state at the transition state geometry, Ψ_L, eq 8. This is the curve annotated with bold circles in Figure 1. In the case of hydrogen transfer process, the bonding combination of the Lewis structures is their negative linear combination (this is typical to all three-electron\three-center systems):[24]

$$\Psi_L = N[\Phi_L(r) - \Phi_L(p)]; \quad N = \text{normalization const.} \quad (8)$$

Further mixing of the foreign excited state into the Lewis state generates the transition state, as defined in eq 9 and shown in Figure 1 by the curve with the bold squares:

$$\Psi_{TS} = c_L\,\Psi_L + c_F\,\Psi_F^*(ct) \quad (9)$$

The Lewis states and the foreign excited states are not frozen and are allowed to relax during the calculations, so that the final adiabatic state (the curve annotated with squares in Figure 1) *is the variational mixture of all of the eight structures in the VB structure set*.

Another important state is the linear combination of the HL structures, which cross along *Q* and thereby generate the backbone of the state crossing in the VBSCD. The bonding combination of the HL structures at the crossing point is called the HL state, given by eq 10:

$$\Psi_{HL} = N[\Phi_{HL}(r) - \Phi_{HL}(p)]; \quad N = \text{normalization const.} \quad (10)$$

It is seen that the Lewis state is fashioned after the HL state. Thus, *although Ψ_{HL} accounts for the covalent three-electron delocalization over the three reaction centers, Ψ_L simply adds the contribution of the ionic fluctuations into the two-electron bonds. The mixing of Ψ_F*(ct) further adds to the transition state the charge-transfer fluctuations from one two-electron bond to the other.*

The involvement of the ionic structures in the transition state is associated with the polar effect which is widely discussed in the physical organic community.[2,3] This effect is measured through Hammett correlations, which characterize the response of probe substituents, on the groups X and/or X′ (taken, e.g., as substituted benzyl groups[2d]), to the electron density development in the transition state. A polar effect in a radical reaction is marked whenever the substituents affect the rate of the reaction in a manner that reveals a significant charge development on the reaction centers. It is apparent that the VB method offers the clearest possible means of defining and quantifying the polar effect by assessing the energetic effect because of the mixing of the ionic structures into the covalent situation, as discussed below.

Computation of Reactivity Parameters. By reference to Figure 1, the important reactivity parameters are the height of the crossing point, ΔE_c, and the resonance energy of the transition states, B. Let us discuss these factors in turn.

The height of the crossing point can be related to the promotion gap separating the two Lewis curves at the extremes of $Q = \pm 1$, as follows:

$$\Delta E_c = fG \tag{11}$$

Thus, G is determined by computing the energies of $\Phi_L(p)$ and $\Phi_L(r)$ at the same geometry corresponds to either $Q = -1$ or to $Q = 1$. The factor f in eq 11 is simply the fraction of the gap that enters under the crossing point, i.e., $f = \Delta E_c/G$, and it is computed variationally during the VB procedure. The third factor in the model is the resonance energy, B, of the transition state. By reference to Figure 1, the B quantity is given by eq 12 as the energy of the transition state relative to the energy of the crossing point; the latter is given by the energy of any one of the Lewis structures at the crossing point:

$$B = |E(\Psi_{TS}) - E(\Phi_{L,cross})| \tag{12}$$

The quantity B provides the resonance energy of the classical Lewis structures and the added contribution of charge-transfer fluctuations (due to the mixing of the Ψ_F*(ct) excited state). B is calculated variationally.

Qualitative Derivation of Reactivity Parameters

Understanding the variation of the reactivity parameters may be achieved by use of a semiempirical VB theory (see Appendix 1) which is based on formally covalent wave functions with embedded ionicity.[25−27]

Promotion Gap. Consider G at $Q = -1$ where X−H is short and H−X′ is infinite. Here, the ground state is $\Phi_L(r)$ having a short X−H bond and an infinitely distant •X′. At the same geometry, $\Phi_L(p)$ is an excited state because the X• •H species in the short linkage are not paired and maintain a nonbonded repulsive interaction, whereas the spin-paired H and X′ species are infinitely distant. It is possible to show that the nonbonded repulsive interactions derive from the Pauli repulsion of two electrons having the same spin, and hence G is related to the singlet−triplet excitation of the X−H bond. In fact, the wave function of the X• •H species is half triplet and half singlet.[8,10] Consequently, the quantity G is simply the energy difference between the ground state with a singlet X−H bond and an excited-state X• •H with a 50% character. With neglect of overlap this becomes

$$G = 0.75\Delta E_{ST}(X-H) = 0.75\Delta E_{ST}(H-X') \tag{13}$$

where the promotion gap is seen to be related to the excitation energy involved in unpairing the X−H electron-pair bond into a triplet pair. The same, but mirror image arguments, exist for the promotion gap at $Q = 1$. Inclusion of overlap changes slightly the factor of 0.75.[28]

The Factor *f*. The semiempirical theory shows that there is a fundamental difference between strong binders and weak binders.[8,9,29] Weak binders are metallic atoms such as alkali which form bonds for which $\Delta E_{ST} \ll 2D$. Strong binders on the other hand form bonds for which $\Delta E_{ST} > 2D$. All of the X groups in our study are strong binders (see later Table 2), and we shall therefore refer only to them in the text (see however the full picture in the Appendix). Thus, the height of the crossing point is $\Delta E_c = 0.25\Delta E_{ST}'$ (the prime refers to the value in the crossing point). Because $G = 0.75\Delta E_{ST}$, then assuming that the $\Delta E_{ST}'$ and ΔE_{ST} values are not too different, the resulting f factor is expected to be a constant in the series, i.e., eq 14:

$$f = \Delta E_c/G \sim 1/3 \tag{14}$$

As shall be seen in the results section, our VBSCDs correspond to the gap expression in eq 13, and the computed f factors are all close to the qualitative estimate in eq 14.

An alternative way to generate the VBSCD would have been to follow the Lewis curves in such a manner that they would have correlated directly to the spectroscopic state in which the unpaired moiety, e.g., X• •H, is in a pure triplet situation, coupled to the distant •X′ into a doublet state,[8,10] in which case the promotion gap G' will be

$$G' = \Delta E_{ST} \tag{15}$$

Because the *variationally determined height of the crossing point* must be the same in the two cases, there will be a mutual compensation in the value of f to ca. $f' \sim 0.25$, to keep the same ΔE_c value. This alternative method although in principle entirely equivalent to the one based on eqs 13 and 14 is more complex to implement in a fully variational manner. Nevertheless, for qualitative discussions we can use either set of quantities: G, f or G', f'.

The B factor: Using the semiempirical VB theory, the quantity B is expected[8,9,29,30] to be eq 16:

$$B = 0.25\Delta E_{ST}' \tag{16}$$

where the primed value refers to the singlet−triplet excitation at the crossing point.

There are a few related quantities, which are qualitatively useful. One is B_L, which is the resonance energy due to only the avoided crossing of the classical Lewis curves, as defined in eq 17a. The second is the resonance energy due to the covalent HL structures only as in eq 17b. Finally, the covalent−ionic resonance energy is defined by eq 17c. The latter quantity provides the complete contribution of the ionic and charge transfer structures relative to the covalent HL state and is associated with the polar effect:[2,3]

$$B_L = |E(\Psi_L) - E(\Psi_{cross})| \tag{17a}$$

$$B_{HL} = |E(\Psi_{HL}) - E(\Phi_{HL,\,cross})| \tag{17b}$$

$$RE_{cov-ion} = |E(\Psi_{TS}) - E(\Psi_{HL})| \tag{17c}$$

All of these values are computed in this study in a manner where the states and the reference structures are variational wave functions.

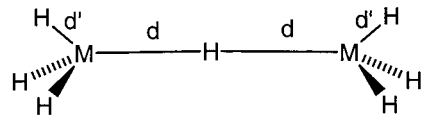

MH_3	d	d'	d_0	$\%(\Delta d/d_0)$
H	0.927	-	0.738	25.6
CH_3	1.334	1.091	1.079	23.6
SiH_3	1.773	1.486	1.483	19.6
SiH_3[a]	1.768	1.482	1.481	19.4
GeH_3[a]	1.834	1.550	1.546	18.9
SnH_3[a]	2.014	1.724	1.719	17.2
PbH_3[a]	2.023	1.755	1.741	16.2

a) ECP-31G*

Figure 3. Optimized (MP2/6-31G* and MP2/ECP-31G*) bond lengths (in Å) of reactants (d_0) and transition states (d and d') for identity hydrogen transfer reactions.

TABLE 1: BOVB Calculated Weights of Covalent (ω_{Cov}) and Ionic (ω_i) Structures[a] in the Ground and Transition State of the $X^{\bullet} + H-X' \rightarrow X-H + {}^{\bullet}X'$ Process

entry	X	ω_{cov} [b]	ω_i(r,p)[b]	ω_i(ex)[b]
1	H	0.700 (0.794)	0.265 (0.206)	0.035 (0.000)
2	CH_3	0.640 (0.723)	0.311 (0.277)	0.049 (0.000)
3	SiH_3	0.584 (0.742)	0.328 (0.258)	0.088 (0.000)
4	SiH_3 [c]	0.628 (0.783)	0.307 (0.217)	0.065 (0.000)
5	GeH_3 [c]	0.634 (0.784)	0.308 (0.216)	0.058 (0.000)
6	SnH_3 [c]	0.635 (0.788)	0.300 (0.212)	0.065 (0.000)
7	PbH_3 [c]	0.637 (0.786)	0.293 (0.214)	0.070 (0.000)

[a] ω_i(r,p) refers to structures **3**−**6**, whereas ω_i(ex) refers to **7** and **8** in Scheme 1. [b] Values out of parentheses are for the transition state. Values in parentheses refer to the reactants. [c] ECP/31G* data. Other data refer to 6-31G*.

From the above derivations, it follows that all of the reactivity factors are related to one quantity: ΔE_{ST}, the singlet−triplet promotion energy of the bond which is broken during the transformation.

Results

Figure 3 shows the key geometric parameters of the species, where d and d' refer to the transition state and d_0 refers to the ground-state molecule. The computation for X= SiH_3 were done at the all electron (ae) as well as effective core potential levels to ascertain the compatibility of the two basis sets. Also shown in the figure is the fraction of bond lengthening in the transition state ($\Delta d/d_0 = [(d - d_0)/d_0]$). It is seen that, as X is varied down the family, the fraction of bond stretching decreases.

Table 1 collects the weights of the covalent (ω_{cov}) and ionic structures (ω_i). The latter are separated into the ionic structures, which contribute to the Lewis bonds ω_i(r,p) and those nascent from the foreign excited charge transfer state, ω_i(ex). The corresponding weights for the reactants are given in parentheses. All of the species are dominated by the covalent structures, but *the transition states are considerably more ionic than the reactants*. The major ionic contribution comes from those structures which contribute to the Lewis bonds, whereas the charge-transfer types have smaller weights. The covalent weight, ω_{cov}, exhibits a zigzag pattern, starting high for X = CH_3, decreasing for X = SiH_3, increasing again for X = GeH_3, and for X = PbH_3. This trend follows the X electronegativity that does not decrease uniformly down the family because of two important effects: One is "the transition metal contraction" which occurs down from Si to Ge, making the latter more electronegative. The second is the "relativistic contraction" which occurs in the transition from Sn to Pb.[31]

Table 2 shows barriers and reactivity quantities at the different VB levels, BOVB and BDOVB. These are compared whenever appropriate to the MP2 and CCSD(T) quantities. The BOVB computed bond energies, D, compare accurately to the MP2 data. The BOVB barriers are closer to the MP2 barriers than the BDOVB values. It is clear though that all of the methods are less accurate than the more extensive CCSD(T) method. The most accurately computed barrier for X = H is ca. 10 kcal/mol.[12] The experimental barrier for X = CH_3 is estimated as 18 kcal/mol[5,32] from the experimental activation energy (14.9 kcal/mol[13,14]). However, what is important is that all of the methods give the same trends, that the barriers decrease down the family from X = CH_3 to PbH_3. It is seen that the trend in the barrier reflects the trend in the percentage of bond stretching in the transition state, in Figure 3. The higher the barrier the more extensive is the bond stretching in the transition state.

The BOVB values of the transition state resonance energy quantity B are about 1 kcal/mol larger than the corresponding BDOVB data. The height of the crossing point differs by approximately 2 kcal/mol for the two methods. These two small increments account together for the almost constant 3.23 ± 0.43 kcal/mol difference in the barriers of the two VB methods. Apparently, the constrained BDOVB wave function exerts a roughly constant effect on all of the reactions, relative to the more flexible BOVB method. It is interesting to note that the B value for X = H is virtually the same as the one reported 11 years ago using a multistructure VB method and a more extensive basis set than here.[8] Indeed, from previous experience with delocalized ground-state species, isoelectronic with the transition states in this study, the accuracy of the B quantity (wherever could be compared with experimental estimates) is generally good at the BOVB level with double-ζ basis set. It is likely therefore that the major source of discrepancy in the barrier, relative to higher level computations, will arise because of overestimation of the height of the crossing point.

The B_L quantity, in Table 2, provides the resonance energy due to the two classical Lewis structures. The $B - B_L$ difference is approximately a constant 6.5 ± 1.2 kcal/mol for all of the series. This rather small difference shows that most of the resonance energy of the transition state is due to the classical Lewis structures and the charge transfer states contribute a smaller amount that appears to be constant in the series.

Further insight into the factors of the resonance energy can be gained from the B_{HL} quantity that refers to the resonance energy of the covalent HL structures alone. It is seen that the covalent resonance energy, which depends largely on the atomic resonance integrals and corresponding overlaps,[24,30] does not vary much in the series. It is largest for X = H and CH_3, reflecting the fact that these are the strongest binders in the series, having the largest resonance integrals. Complementary to the covalent resonance energy is the covalent−ionic resonance energy, $RE_{cov-ion}$ defined above in eq 17c. It is seen again that $RE_{cov-ion}$ is roughly a constant, with the exception of CH_3 which has the largest contribution. Moreover, the $RE_{cov-ion}$ does not correlate with the weight of the ionic structures, in Table 1, which are seen to be larger for the heavier elements in the series. The reason for that is that the ionic−covalent contribution to the resonance energy of the transition state is a perturbation by the ionic structures on the primary covalent HL state. The

TABLE 2: Barriers and VB Quantities for $X^{\bullet} + H-X' \rightarrow X-H + {}^{\bullet}X'$ [a]

		H	CH_3	SiH_3	SiH_3 [b]	GeH_3 [b]	SnH_3 [b]	PbH_3 [b]
$\Delta E^{\ddagger}$	MP2	17.7	22.3	16.5	16.1	13.6	10.5	8.5
	CCSD(T)	14.9	21.4		14.7	11.1	10.2	7.6
	BOVB	17.8	23.1	19.1	21.2	18.1	15.0	12.3
	BDOVB	20.6	26.2	22.5	25.4	21.7	17.9	14.9
	Exptl.	≈10	14.7 (18)					
D	MP2	92.6	103.9	84.2	85.2	77.6	68.3	61.6
	VB	93.9	99.5	84.9	85.5	78.3	70.2	63.9
B	BOVB	42.9	51.1	38.8	41.5	38.5	33.3	31.8
	BDOVB	41.8	50.2	37.6	39.7	37.4	32.7	31.4
ΔE_c	BOVB	60.6	74.2	57.9	62.6	56.6	48.3	44.1
	BDOVB	62.4	76.4	60.1	65.1	59.1	50.6	46.3
G	BOVB	163.9	192.9	144.3	158.6	145.7	124.2	115.8
ΔE_{ST}	BOVB	240.3	276.4	234.0	224.2	212.0	187.5	172.1
$G/\Delta E_{ST}$	BOVB	0.68	0.70	0.62	0.71	0.69	0.66	0.67
f	BOVB	0.37	0.38	0.40	0.40	0.39	0.39	0.38
B_L	VB	35.8	41.2	33.3	34.7	32.4	28.1	26.4
B_{HL}	VB	28.0	32.1	26.8	26.0	25.4	21.8	21.2
$RE_{cov-ion}$	BOVB	20.5	35.3	23.2	24.5	22.7	20.7	20.3

[a] In kcal/mol. [b] ECP-31G*.

covalent-ionic resonance energy can then be expressed as a sum of the perturbation energies of the individual ionic structures, as shown in eq 18:

$$RE_{cov-ion} = \Sigma_i \delta E_{cov-ion}(i) = \Sigma_i c_i \langle \Phi_i | \mathbf{H} | \Psi_{HL} \rangle \qquad (18)$$

Here, c_i is the coefficient of the ith ionic structure and the second factor is the matrix element of that structure with the HL state. The matrix element is proportional to the resonance integrals between X and H. These resonance integrals are larger for the lighter element, C, in the $X = MH_3$ series (M = C, Si, Ge, Sn, and Pb) which is also the stronger binder. The coefficient c_i is inversely proportional to the energy gap between the ionic structure and the HL state. This gap decreases for the heavier elements in the series, so they have higher degree of ionicity in the transition state. However, the contribution $\delta E_{cov-ion}(i)$ to the covalent−ionic resonance energy, which is a product of two oppositely varying quantities, remains quasiconstant, with the exception of $X = CH_3$ where the matrix element appears to dominate the behavior of all of the components of the resonance energy (B_L, B_{HL}, and $RE_{cov-ion}$) in Table 2.

The other quantities in Table 2 are G, ΔE_{ST}, and f. First, it is seen that the bond energy is related to the singlet−triplet excitation as, $D = 0.36 - 0.48\Delta E_{ST}$, such that all of the groups are strong binders with $\Delta E_{ST} > 2D$. The promotion gaps, G, is almost a constant fraction 0.69−0.71 of the singlet−triplet excitation of the bond, ΔE_{ST}, as predicted in eq 13. The f factor is a quasiconstant close to the predicted value, $^1/_3$ in eq 14, using qualitative reasoning of semiempirical VB theory. As reasoned above, an alternative VBSCD would contain principal Lewis curves anchored in spectroscopic states with $G' = \Delta E_{ST}$ (eq 15). To produce the same height of the crossing point, ΔE_c, the f quantity would be rescaled by a constant factor of 0.69−0.71, which is found to exist here between G and ΔE_{ST}. These scaled f' values will also be quasiconstant, 0.25−0.27, in accord with the qualitative estimate. Indeed, as stated already above, the two alternative VB diagrams would lead to entirely equivalent predictions.

Discussion

Figure 4 shows the correlation of the barrier, $\Delta E^{\ddagger}$, the height of the crossing point, ΔE_c, and transition state's resonance energy, B, against three fundamental quantities: the promotion gap, G, in (a), the singlet−triplet excitation of the activated bond, ΔE_{ST}, in (b), and the bond energy of this bond, D, in (c). The correlations look almost identical due to the fact, already reasoned above, that both G and D vary in relation to the ΔE_{ST} quantity of the bond undergoing activation. Moreover, it appears that the major reactivity factors ΔE_c and B also correlate with the ΔE_{ST} quantity. In the following discussion, we formulate simple expressions which enable one to estimate the barrier in a manner that reveals the interrelation of all of the quantities.

A. Qualitative vis a vis Quantitative Aspects of the VBSCD. Table 3 involves barriers calculated by model VB equations based on the semiempirical derivations of the various VB factors. The expressions of the barriers rely on singlet−triplet excitation energies. Because the latter quantities are not always readily available, we derive alternative expressions based on bond energies, via the relation of the latter quantities to the singlet−triplet excitations.

Resonance Energy of the Transition State. We start with the resonance energy of the transition state, B. On the basis of eq 16, B is one-quarter of the singlet−triplet excitation energy, $\Delta E_{ST}'$, of the X−H bond at the transition state. Because the transition state bonds are stretched, the $\Delta E_{ST}'$ values are smaller than the corresponding ones, ΔE_{ST}, at the reactant geometry. We may therefore express B in terms of the ΔE_{ST} quantity as follows:

$$\Delta E_{ST}' = (1-\kappa)\Delta E_{ST} \qquad (19a)$$

$$B = 0.25\Delta E_{ST}' = 0.25(1-\kappa)\Delta E_{ST} \qquad (19b)$$

Using the B datum for X = H, we obtain from eq 19b a value of $\kappa = 0.28$, whereas for the entire series, the values cluster near a constant, $\kappa = 0.29-0.26$. We therefore carry $\kappa = 0.28$ as a constant for the series to obtain the values in Table 3. These B values compare very well with the VB computed ones. It is interesting to note that the value $\kappa = 0.28$ corresponds very closely to the fraction of bond stretching, $\Delta d/d_0$, in the transition state (0.26 for X = H), so that one may replace κ by $\Delta d/d_0$ and consider that $\Delta E_{ST}'$ decreases linearly as $\Delta d/d_0$ increases. Using the $\Delta d/d_0$ values from Figure 3 leads to a set of B values (not shown) which are nearly as good as the ones presented in Table 3 using a constant κ.

The second column in Table 3 lists B values estimated from the bond energy, in eq 20:

$$B = 0.5D \qquad (20)$$

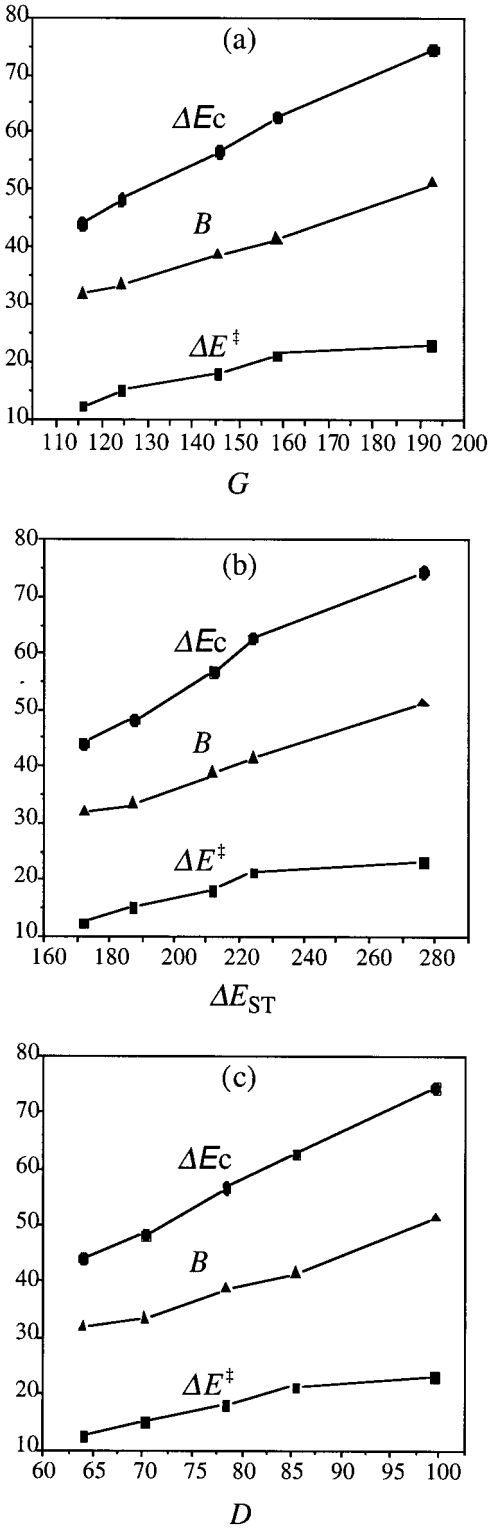

Figure 4. Correlations of the barriers ($\Delta E^{\ddagger}$), heights of the crossing point (ΔE_c), and transition state resonance energies (B) in (a) with the promotion energy gaps, in (b) with the singlet−triplet excitation energy, and in (c) with the bond energy. All data for X = SiH_3 refer to ECP-31G*.

The logic behind this expression relies on the fact that at the geometry of the reactants $\Delta E_{ST} > 2D$. Because at the transition state geometry $\Delta E_{ST}'$ gets smaller because of bond stretching, we may set $\Delta E_{ST}' \sim 2D$, and the equation for B follows from the relation in eq 19b. Once again, the so calculated *B quantities* are nearly as good as the VB computed ones (see Table 3).

TABLE 3: Model and Computed Quantities for $X^{\bullet} + H-X' \rightarrow X-H + {}^{\bullet}X'$

	B, kcal mol^{-1}			$\Delta E^{\ddagger}$, kcal mol^{-1}		
X	eq 19b	eq 20	BOVB	eq 21	eq 22	BOVB (MP2; CCSD(T))
H	43.3	47.0	42.9	16.8	15.7	17.8 (17.7; 14.9)
CH_3	49.8	49.8	51.1	19.3	16.6	23.1 (22.3; 21.4)
SiH_3	40.4	42.8	41.5	15.7	14.3	21.2 (16.1; 14.7)
GeH_3	38.2	39.2	38.5	14.8	13.1	18.1 (13.6; 11.1)
SnH_3	33.8	35.1	33.3	13.1	11.7	15.0 (10.5; 10.2)
PbH_3	31.0	31.9	31.8	12.0	10.7	12.3 (8.5; 7.6)

Barrier Heights. Having expressions for B, the barrier can then be estimated from the barrier equation where the height of the crossing point is expressed as a fraction of either the singlet−triplet excitation ΔE_{ST}, or of the corresponding bond energy D.

Using $G = 0.75\Delta E_{ST}$ (eq 13) and the qualitatively derived f value of $^1/_3$ (eq 14), the height of the crossing point becomes $\sim 0.25\Delta E_{ST}$, and in combination with the expression for B in eq 19b, the barrier expression follows:

$$\Delta E^{\ddagger} = 0.25\kappa\Delta E_{ST}; \quad \kappa = 0.28 \tag{21}$$

Using the computed relation between the bond energy and the singlet−triplet excitation, $D = (0.37 - 0.38)\Delta E_{ST}$, we get $G \sim 2D$. Together with the B expression in eq 20, the corresponding expression for the barrier follows then in terms of bond energy only:

$$\Delta E^{\ddagger} = (2f - 0.5)D; \quad f = 1/3 \tag{22}$$

The so calculated barriers are presented in Table 3 alongside the VB, MP2, and CCSD(T) barriers. The simple expressions for the barrier seem to capture the essence in the computed trends. For X = H and CH_3, the model barriers are closer to CCSD(T) barriers and experimental data than either the VB or MP2 data. If instead of the qualitatively derived f value we use in eq 22 the computed value, $f = 0.37$, we obtain another set of barriers which are close to the VB computed values. This shows consistency of the barrier equations. This consistency further supports our statement above that the B quantity is accurate while most of the VB error in the calculation comes from overestimation of the height of the crossing point, through f. Furthermore, all of the expressions starting with eq 19 through to eq 22 project the root cause of the interrelationship between all of the quantities as revealed by the plot in Figure 4. Thus, *the singlet−triplet excitation of the X−H bond that undergoes activation is the organizing quantity of all of the trends in the series.* The ionic structures seem to have a constant, albeit significant, effect on all of the barriers in this particular series. Thus, although the polar effect on the identity barriers exists, it is concealed because of its quasiconstant behavior.

Related Trends. To test the usefulness of eqs 21 and 22 for predicting barrier heights in identity hydrogen transfer reactions, we applied them to two other series.

Pross et al.[5] studied the hydrogen abstraction barriers in the identity process of alkyl radicals (R = R′ = CH_3, C_2H_5, *i*-C_3H_7, and *t*-C_4H_9):

$$R^{\bullet} + H-R' \rightarrow R-H + R'^{\bullet} \tag{23}$$

They observed a decrease of the barrier as the C−H bond became weaker and explained the trend in precisely the same manner as in the present paper. Using their computed barriers and the corresponding bond energies, it is possible to fit the

TABLE 4: Model and Computed Quantities for $X^{\bullet} + H-X' \rightarrow X-H + {}^{\bullet}X'$

X	$\Delta E^{\ddagger}$ (eq 22)[a]	$\Delta E^{\ddagger}$ (CCSD(T))[a,b]
F	22.7	22.2 (23.9)[c]
Cl	17.2	15.6
Br	14.6	11.3
I	11.9	

[a] In kcal mol^{-1} [b] CCSD(T)/6-31++G* [c] Reference 35 at the DZP/CI level.

barriers with good accuracy to the general expression in eq 3 and obtain eq 24:

$$\Delta E^{\ddagger} = 0.3481G - 50.0 \text{ kcal/mol}; \quad G = 2D_{C-H} \quad (24)$$

Here, the f value is quite close the semiempirical $f = {}^1/_3$ estimate (eq 14). The resonance energy of the transition state is 50 kcal/mol which is close to the value computed in our study for $X = X' = CH_3$ (Table 2). Furthermore, B behaves as a constant in the series. If we allow the value of B to vary with the value of D, as in eq 20, we can still reproduce the trend in these barriers, but the scale of the barriers would now be much more condensed than the scale in eq 24. This means in turn that, when all of the atomic centers of the reaction remain the same, the quantity B can be treated as a constant too. It is certain that the weight of transition state ionicity increases in the series as the ionization energy of X and X′ decreases from $R = R' = CH_3$ to $R = R' = t\text{-}C_4H_9$. We may surmise therefore that in this series the increase of ionicity contributes to the transition state resonance energy in a manner that levels the falloff because of reduction in the bond energy. The end result of the constancy of B in eq 24, imparted by the polar effect, is that the reactivity trends in the series is dominated by the promotion gap (i.e., the singlet−triplet excitation).

An interesting series is the identity hydrogen transfer between electronegative atoms, in eq 25:

$$X^{\bullet} + H-X' \rightarrow X-H + X'^{\bullet}; \quad X = X' = \text{F, Cl, Br, and I} \quad (25)$$

A good reason to consider this series is that the X and X′ groups are electronegative, and therefore, one might expect significant contribution of bond ionicity effects, in accord with the well established polar effect in hydrogen abstractions.[2−4] The barriers in this series were addressed by experimentalists and theoreticians, and the consensus is that the barrier decreases in moving from F toward I.[33,34] Application of eq 22, using the known bond energies of the H−X molecules, leads to the barriers in Table 4. The barriers compare well with the CCSD(T) data. The barrier calculated by the model for $X = X' = F$ is also in good agreement with the datum of Schaefer et al. is 23.9 kcal/mol.[35] In fact, the barriers in Tables 2 and 3 enable us to assess the model equation's ability to predict trends along a row of the priodic table. Thus, eq 22 predicts, in accord with the results of CCSD(T), that in each row the identity barrier is generally larger for the more electronegative groups, X and X′ (compare, e.g., the barriers for $X = F$ vs CH_3, etc).

All in all, the correspondence of the estimated barriers to the computed data are very good. Apparently, in this identity series too, the polar effect is masked. Thus, the decrease of the B value in the series (through the expression in eq 20) follows the decrease of bond energy, and this in turn follows the decrease of electronegativity in the series. So, although the ionicity effect is significant in the absolute sense, as we saw for the target series studied here by VB, the effect is either constant in the series or it varies with the other parameters in a uniform manner. The net result is that again the promotion gap (or D through its relation to G) dominates the trends in the series. It is no wonder therefore that a great deal of reactivity patterns in hydrogen abstraction are dominated by bond strength effects, even in reactions of transition metal oxidants such as MnO_4^-, CrO_2Cl_2, etc.[36] This however does not rule out the importance of the well-known polar effect,[2,3] as demonstrated recently by in the computational studies of Hrovat and Borden[3b] and Fox and Schlegel.[3a] A two-state modeling by Donahue et al.[4] projects the importance of ionicity. Similarly, polar effects are evident in radical additions to olefins as revealed by ab initio computations and VB modeling by Wong et al.,[37] Fischer et al.,[7] and Fischer and Radom.[38] However, what appears from all of these studies is that the polar effect is expressed more clearly in hydrogen transfers between nonidentical groups (nonidentity reactions). In identity reactions as the ones studied here, the polar effect is masked and the organizing quantity remains the singlet−triplet promotion gap.

Equations 22 and 23 are limited to identity hydrogen abstraction by strong binders. However, the VBSCD model in its general form, is applicable to transfers of other atoms of the general $X + X-X'$ type.[8,10] One of the interesting predictions that the model makes is that when the X becomes a weak binder, D becomes small, and $\Delta E_{st} \ll 2D$ the barrier becomes negative and the X−X−X species becomes a stable cluster along the exchange coordinate (see derivation in Appendix 1). This was shown before by Malrieu.[29] A typical such situation is when X changes from X = H which is a strong binder to X = Li which is a weak binder (X = H, $D = 93.9$, $\Delta E_{st} = 240$ kcal/mol; X = Li, $D = 25$ kcal/mol and $\Delta E_{st} = 32.9$ kcal/mol) the X_3 cluster changes from a transition state to a stable entity for X = Li. *Thus, the singlet−triplet promotion gap is the organizing quantity which predicts also the global change in the nature of (X−X−X)· clusters as X changes from a nonmetal to a metallic species.*

Conclusions

The paper applies VB computations to obtain identity barriers for hydrogen transfer reactions between X groups, $X = X' = CH_3$, SiH_3, GeH_3, SnH_3, and PbH_3. Modeling of these barriers by means of VB state correlation diagrams (VBSCDs) leads to simple expressions for the barriers, in eqs 21 and 22. These expressions show that the organizing quantity of the barriers is the singlet−triplet excitation energy (ΔE_{ST}) or bond energy (D) of the X−H bond that undergoes activation. The larger the ΔE_{ST} or D, the higher the identity barrier. These equations are successfully applied to deduce barriers for hydrogen transfers between electronegative groups, $X = X' = F$, Cl, Br, and I. The polar effect is shown to be significant but virtually constant in the series. Thus, identity processes mask the polar effect, which is more clearly expressed in nonidentity hydrogen transfer reactions.

The model (though not the specific parameters) is applicable to other atom transfer reactions where the Lewis bond, polar as it may be, is still dominated by the covalent VB structure. In such a case, the curves of the VBSCD are anchored in covalent states and the promotion gap is given by the singlet−triplet excitation energy. The model predicts that as the ratio of the singlet−triplet excitation to the bond energy decreases below a critical value, the saddle-point will be transformed to a stable minimum along the exchange coordinate.[8,10]

In atom transfer reaction where the bond wave function is dominated by ionic structures, the VBSCD will be transformed into one where the principal curves are anchored in the charge transfer states (Ψ_F* in this study).[10] In such a reaction series, reactivity will be dominated by redox properties of the reactants, as already noted for the C−F bond activation in the F-abstraction reactions of lanthanide cations, $Ln^+ + R-F$.[10,39] Thus, atom transfer reactions will exhibit the gamut of reactivity patterns from the covalent regime to ionic one.

Acknowledgment. The research at HU is supported by the VW Stiftung through the Ministry of Sciences of the Niedersachsen States. The research at XMU is supported by the Natural Science Foundation of China (Nos. 20073033 and 29892166).

Appendix

Semiempirical VB treatments of the three-electron problem have appeared before.[8,29] The dependence of G and B on ΔE_{ST} (eqs 13 and 16) and the values for f (eq 14) were derived and appear in refs, 8, 9, 28, and 30. This appendix uses expressions based on the recent semiempirical approach of Wu et al.[26] The elements of this approach are similar in essence to the seminal treatment of Malrieu in terms of a Heisenberg Hamiltonian.[29]

The energy of a Lewis bond, e.g., H−X (or X−X) relative to the nonbonded reference determinant[26,40] is given by:

$$E_S(H-X) = -\lambda; \quad D(H-X) = \lambda \tag{A.1}$$

Neglecting overlap in the normalization factors of the wave functions, the energy of the triplet pair H• •X (or of X• •X) is also $+\lambda$. However, this identity of expressions assumes that the orbitals of the singlet paired bond (eq A.1) and of the triplet pair are the same. This needs not be true, and the triplet pair will have its own set of orbitals with energy in eq A.2:

$$E_T(H\bullet\ \bullet X) = \lambda_T \tag{A.2}$$

The singlet−triplet excitation becomes then eq A.3. The expressions for G and B follow in eqs A.4 and A.5, where the primed quantities refer to the values at the crossing point of the VBSCD (Figure 1)

$$\Delta E_{ST}(H-X) = (\lambda + \lambda_T) \tag{A.3}$$

$$G = 0.75\Delta E_{ST}(H-X) = 0.75(\lambda + \lambda_T) \tag{A.4}$$

$$B = 0.25\ \Delta E_{ST}'(H-X) = 0.25(\lambda' + \lambda_T') \tag{A.5}$$

At the crossing point (Figure 1) the Lewis structure, X• H−X has on one side a bond with energy $-\lambda'$ and half a repulsive interaction on the other side with energy $0.5\lambda_T'$.[26] Thus the energy of the crossing point is given by

$$E_c(X\bullet\ H-X) = -\lambda' + 0.5\lambda_T' \tag{A.6}$$

To enable us to derive a simple expression for the barrier, we assume that $\lambda = \lambda'$. With this assumption, the height of the crossing point becomes eq A.7:

$$\Delta E_c = 0.5\ \lambda_T \tag{A.7}$$

This expression shows that the height of the crossing point depends on the triplet repulsive interactions between the bonded atom in the center (e.g., H) and the two terminal groups X.

The f factor becomes then eq A.8:

$$f = \Delta E_c/G = \{2\alpha/[3(1+\alpha)]\}; \quad \alpha = \lambda_T/\lambda \tag{A.8}$$

Combining equations A.8, A.7, A.5, and A.4, the barrier expression becomes

$$\Delta E^{\ddagger} = 0.25\Delta E_{ST}\,[(\alpha - 1)/(\alpha + 1)] \tag{A.9}$$

It is seen from eq A.9 that the barrier is positive as long as $\alpha > 1$. When $\alpha < 1$, the barrier becomes negative, and the delocalized three-electrons\three-centers species XHX (or X−X−X) becomes a stable cluster along the exchange coordinate (Q in Figure 1).

The parameter α is the crucial quantity that determines the transition from a saddle-point species to a stable cluster. From eqs A.1 and A.3, we can show that α determines the ratio of the singlet−triplet excitation of the bond to its bond energy:

$$\Delta E_{ST}/D = (\lambda + \lambda_T)/\lambda = 1 + \alpha \tag{A.10}$$

All of the X−H bonds in our study are typified by $\Delta E_{ST}/D > 2$ and hence their α values are larger than 1. These are the "strong binders". In contrast, in a bond like Li_2, $\Delta E_{ST} = 32.9$ kcal/mol and $D = 24.6$ kcal/mol, and hence $\alpha = 0.3374$. This is the class of "weak binders", in which the triplet repulsion (λ_T) is significantly shallower than the bonding interaction ($-\lambda$). Equation A.9 predicts that clusters of "weak binders" will be stable intermediates, in contrast to clusters of "strong binders" which are transition states.

Equation A.9 turns out to be useful also for calculating barriers, provided the ΔE_{ST} and α quantities are available. For the target reactions in the paper all of these quantities are available and are displayed in Table 5 along with the corresponding barriers. The results are amazingly good considering the crude nature of the approximation. Assessment of the approximations in terms of the original quantities of the model, G, B, and f, shows that eq A.9 overestimates both B and f and leads to error cancellation.

TABLE 5: ΔE_{ST}, α, and Barriers ($\Delta E^{\ddagger}$) Calculated with eq A.9 for X• + H-X′ → X-H + •X′

X	ΔE_{ST}[a]	α	$\Delta E^{\ddagger}$ (eq A.9)[a]	$\Delta E^{\ddagger}$ (CCSD(T))[a]
H	240.3	1.559	13.1	14.8
CH_3	276.4	1.778	19.4	21.4
SiH_3	224.2	1.622	13.3	14.7
GeH_3	212.0	1.708	13.9	11.1
SnH_3	187.5	1.671	11.8	10.2
PbH_3	172.1	1.693	11.1	7.6
Li[b]	32.9	0.3374	−4.1	−3.8[c]

[a] In kcal mol^{-1}. [b] This corresponds to Li + Li−Li′ → Li−Li + Li′. [c] This is a VB datum from ref 8.

References and Notes

(1) (a) Borman, S. *Chem. Eng. News* **1994**, April 18, 4. (b) See, for example: Giese, B.; Graph, X. B.; Burger, J.; Kesselheim, J.; Senn, M.; Schäfer, T. *Angew. Chem. Int. Ed.* **1993**, *32*, 1742. (c) See, for example: Groves, J. T. *J. Chem. Educ.* **1985**, *62*, 928−931.

(2) (a) For an example of bond energy and polar effects in hydrogen abstraction, see: Sharter, A. B.; Tian, F.; Dolbier, W. R., Jr.; Smart, B. E. *J. Am. Chem. Soc.* **1999**, *121*, 7335. (b) For the first intepretation of polar effects, see: Russell, G. A. *J. Org. Chem.* **1958**, *23*, 1407. (c) Walling, C. *Free radicals in Solution*; Wiley: New York, 1973; Chapter 8. (d) Russell, G. A. In *Free Radicals*; Kochi, J. K., Ed.; Wiley: New York, 1973; Vol 1, pp 293−298.

(3) For some recent computational treatments which exhibit polar effects, see: (a) Fox, G. L.; Schlegel, H. B. *J. Phys. Chem.* **1992**, *96*, 298. (b) Hrovat, D. A.; Bordern, W. T. *J. Am. Chem. Soc.* **1994**, *116*, 6459.

(4) (a) Donahue, M. N.; Clarke, J. S.; Anderson, J. G. *J. Phys. Chem. A* **1998**, *102*, 3923. (b) Clarke, J. S.; Rypkema, H. A.; Kroll, J. H.; Donahue, M. N.; Anderson, J. G. *J. Phys. Chem. A* **2000**, *104*, 4458.

(5) Pross, A.; Yamataka, H.; Nagase, S. *J. Phys. Org. Chem.* **1991**, *4*, 135.

(6) Balint-Kurti, G. G.; Benneyworth, P. R.; Davis, M. J.; Williams, I. H. *J. Phys. Chem.* **1992**, *96*, 4346.

(7) Salikhov, A.; Fischer, H. *Theor. Chim. Acta* **1997**, *96*, 114.

(8) Maitre, P.; Hiberty, P. C.; Ohanessian, G.; Shaik, S. *J. Phys. Chem.* **1990**, *94*, 4089.

(9) Shaik, S.; Hiberty, P. C. In *Theoretical Models for Chemical Bonding*; Maksic, Z. B., Ed.; Springer-Verlag: Heidelberg, Germany, 1991; Vol. 4, p 269.

(10) Shaik, S.; Shurki, A. *Angew. Chem.* **1999**, *38*, 586.

(11) For modeling in terms of the BEBO approach, see: (a) Johnston, H. S.; Parr, C. *J. Am. Chem. Soc.* **1963**, *85*, 2544. (b) Dunning, T. H. *J. Phys. Chem.* **1984**, *88*, 2469. (c) Dunning, T. H., Jr.; Harding, L. B.; Bair, R. A.; Eades, R. A.; Shepard, R. L. *J. Phys. Chem.* **1986**, *90*, 344.

(12) (a) Truhlar, D. G.; Horowitz, J. C. *J. Chem. Phys.* **1978**, *68*, 2466. (b) Siegbahn, P.; Liu, B. *J. Phys. Chem.* **1978**, *68*, 2457.

(13) Creak, G. A.; Dainton, F. S.; Ivin, K. J. *Trans. Faraday Soc.* **1962**, *58*, 326.

(14) Dainton, F. S.; Ivin, K. J.; Willkinson, F. *Trans. Far. Soc.* **1959**, *55*, 926.

(15) Yu, X.; Li, S.-M.; Li, Z.-S.; Sun, C.-C. *J. Phys. Chem. A* **2000**, *104*, 9207.

(16) (a) Hiberty, P. C.; Flament, J. P.; Noizet, E. *Chem. Phys. Lett.* **1992**, *189*, 259. (b) Hiberty, P. C.; Humbel, S.; Byrman, C. P.; Van Lenthe, J. H. *J. Chem. Phys.* **1994**, *101*, 5969. (c) Hiberty, P. C.; Humbel, S.; Archirel, P. *J. Phys. Chem.* **1994**, *98*, 11697. (d) Hiberty, P. C. In *Modern Electronic Structure Theory and Applications in Organic Chemistry*; Davidson, E. R., Ed.; World Scientific: River Edge, NY, 1997; pp 289−367.

(17) Mo, Y.; Lin, Z.; Wu, W.; Zhang, Q. *J. Phys. Chem.* **1996**, *100*, 11569.

(18) Cooper, D. L.; Gerratt, J.; Raimondi, M. *Chem. Rev.* **1991**, *91*, 929.

(19) Goddard, W. A., III; Harding, L. B. *Annu. Rev. Phys. Chem.* **1978**, *29*, 363.

(20) Chirgwin, H. B.; Coulson, C. A. *Proc. R. Soc. London, Ser. A* **1950**, *2*, 196.

(21) Wu, W.; Song, L.; Mo, Y.; Zhang, Q. XIAMEN99−An Ab Initio Spin-Free Valence Bond Program; Xiamen University: Xiamen, P. R. of China, 1999.

(22) Frisch, M. J.; Trucks, G. W.; Schlegel, H. B.; Scuseria, G. E.; Robb, M. A.; Cheeseman, J. R.; Zakrzewski, V. G.; Montgomery, J. A., Jr.; Stratmann, R. E.; Burant, J. C.; Dapprich, S.; Millam, J. M.; Daniels, A. D.; Kudin, K. N.; Strain, M. C.; Farkas, O.; Tomasi, J.; Barone, V.; Cossi, M.; Cammi, R.; Mennucci, B.; Pomelli, C.; Adamo, C.; Clifford, S.; Ochterski, J.; Petersson, G. A.; Ayala, P. Y.; Cui, Q.; Morokuma, K.; Malick, D. K.; Rabuck, A. D.; Raghavachari, K.; Foresman, J. B.; Cioslowski, J.; Ortiz, J. V.; Stefanov, B. B.; Liu, G.; Liashenko, A.; Piskorz, P.; Komaromi, I.; Gomperts, R.; Martin, R. L.; Fox, D. J.; Keith, T.; Al-Laham, M. A.; Peng, C. Y.; Nanayakkara, A.; Gonzalez, C.; Challacombe, M.; Gill, P. M. W.; Johnson, B. G.; Chen, W.; Wong, M. W.; Andres, J. L.; Head-Gordon, M.; Replogle, E. S.; Pople, J. A. *Gaussian 98*; Gaussian, Inc.: Pittsburgh, PA, 1998.

(23) Heitler, W.; London, F. *Z. Physik* **1927**, *44*, 455.

(24) Shaik, S. S. In *New Concepts for Understanding Chemical reactions*; Bertran, J., Csizmadia, I. G., Eds.; ASI NATO Series, *C267*; Kluwer Publ.: Dordrecht, The Netherlands, 1989; p 165.

(25) Wu, W.; Zhong, S.-J.; Shaik, S. *Chem. Phys. Lett.* **1998**, *292*, 7−14.

(26) Wu, W.; Danovich, D.; Shurki, A.; Shaik, S. *J. Phys. Chem. A* **2000**, *104*, 8744.

(27) Using BDOs, the wave function is formally covalent and the ionicity is embedded through the delocalization tails. See, e.g.: Hiberty, P. C. *J. Mol. Struct. (THEOCHEM)* **1998**, *451*, 237.

(28) Shaik, S. S.; Hiberty, P. C.; Lefour, J. M.; Ohanessian, G. *J. Am. Chem. Soc.* **1987**, *109*, 363.

(29) Malrieu, J. P. *Nouv. J. Chim.* **1986**, *10*, 61.

(30) Shaik, S.; Duzy, E.; Bartuv, A. *J. Phys. Chem.* **1990**, *94*, 6574.

(31) Pyykkö, P. *Chem. Rev.* **1988**, *88*, 563. (b) Pyykkö, P. *J. Chem. Res. (S)* **1979**, 380.

(32) Wildman, T. A. *Chem. Phys. Lett.* **1986**, *126*, 325.

(33) Parr, C. A.; Truhlar, D. G. *J. Phys. Chem.* **1971**, *75*, 1844.

(34) Last, I.; Baer, M. *J. Chem. Phys.* **1984**, *80*, 3246.

(35) O'Niel, S. V.; Schaefer, H. F., III; Bender, C. F. *Proc. Natl. Acad. Sci. U.S.A.* **1974**, *71*, 104.

(36) Mayer, J. M. Thermodynamic Influence on C−H Bond Oxidation. In *Biomimetic Oxidations Catalyzed by Transition Metal Complexes*; Meunier, B., Ed; Imperial College Press: London, 1999; Chapter 1.

(37) Wong, M. W.; Pross, A.; Radom, L. *J. Am. Chem. Soc.* **1993**, *115*, 11050; *Isr. J. Chem.* **1993**, *33*, 415; *J. Am. Chem. Soc.* **1994**, *116*, 11938.

(38) Fischer, H.; Radom, L. *Angew. Chem.* **2001**, *40*, 1340.

(39) Cornehl, H. H.; Hornung, G.; Schwarz, H. *J. Am. Chem. Soc.* **1996**, *118*, 9960. (b) Harvey, J. N.; Schröder, D.; Koch, W.; Danovich, D.; Shaik, S.; Schwarz, H. *Chem. Phys. Lett.* **1997**, *278*, 391.

(40) The reference determinant is one in which the spins alternate (up and down) but are not paired. The energy of this reference state does not vary with the distance between the atoms and hence it is a nonbonded state. See: (a) Hiberty, P. C.; Danovich, D.; Shurki, A.; Shaik, S. *J. Am. Chem. Soc.* **1995**, *117*, 7760. (b) Galbraith, J. M.; Blank, E.; Shaik, S.; Hiberty, P. C. *Chem. Eur. J.* **2000**, *6*, 2425.